J|A|C|S
ARTICLES
Published on Web 10/06/2006

Nonlinear Optical Properties and Excited-State Dynamics of Highly Symmetric Expanded Porphyrins

Zin Seok Yoon,[†] Jung Ho Kwon,[†] Min-Chul Yoon,[†] Mi Kyoung Koh,[†] Su Bum Noh,[†] Jonathan L. Sessler,*[,‡] Jeong Tae Lee,[‡] Daniel Seidel,[‡] Apolonio Aguilar,[‡] Soji Shimizu,[§] Masaaki Suzuki,[§] Atsuhiro Osuka,*[,§] and Dongho Kim*[,†]

Contribution from the Department of Chemistry and Center for Ultrafast Optical Characteristics Control, Yonsei University, Seoul 120-749, Korea, Department of Chemistry and Biochemistry, 1 University Station, A5300, The University of Texas at Austin, Austin, Texas 78712-0165, and Department of Chemistry, Graduate School of Science, Kyoto University, and Core Research for Evolutional Science and Technology (CREST) of Japan Science and Technology Agency (JST), Kyoto 606-8502, Japan

Received July 5, 2006; E-mail: dongho@yonsei.ac.kr; sessler@mail.utexas.edu; osuka@kuchem.kyoto-u.ac.jp

Abstract: A strong correlation among calculated Nucleus-Independent Chemical Shift (NICS) values, molecular planarity, and the observed two-photon absorption (TPA) values was found for a series of closely matched expanded porphyrins. The expanded porphyrins in question consisted of [26]hexaphyrin, [28]-hexaphyrin, rubyrin, amethyrin, cyclo[6]pyrrole, cyclo[7]pyrrole, and cyclo[8]pyrrole containing 22, 24, 26, 28, and 30 π-electrons. Two of the systems, [28]hexaphyrin and amethyrin, were considered to be antiaromatic as judged from a simple application of Hückel's $[4n + 2]$ rule. These systems displayed positive NICS(0) values (+43.5 and +17.1 ppm, respectively) and gave rise to TPA values of 2600 and 3100 GM, respectively. By contrast, a set of congeners containing 22, 26, and 30 π-electrons (cyclo[n]pyrrole, $n = 6$, 7, and 8, respectively) were characterized by a linear correlation between the NICS and TPA values. In the case of the oligopyrrolic macrocycles containing 26 π-electron systems, a further correlation between the molecular structure and various markers associated with aromaticity was seen. In particular, a decrease in the excited state lifetimes and an increase in the TPA values were seen as the flexibility of the systems increased. Based on the findings presented here, it is proposed that various readily measurable optical properties, including the two-photon absorption cross-section, can provide a quantitative experimental measure of aromaticity in macrocyclic π-conjugated systems.

Introduction

Expanded porphyrins, including inter alia oligopyrrolic macrocycles containing more than four pyrrole rings, have attracted considerable attention recently because of their potential utility in applications such as medicine, sensor development, and catalysts.[1−4] These systems also provide a test bed in which issues of aromaticity in large heteroannulenes may be explored. Such studies are of fundamental interest, not only on a theoretical level but also on a practical one because they allow predictions of new, potentially interesting synthetic targets to be made with greater confidence.[5] Unfortunately, to date, chemical characterizations of expanded porphyrins have been largely limited to structural studies involving X-ray diffraction methods, as well as UV−vis, NMR, and MCD spectroscopic analyses. While this has provided considerable insight into the

[†] Yonsei University.
[‡] The University of Texas at Austin.
[§] Kyoto University.

(1) (a) Jasat, A.; Dolphin, D. *Chem. Rev.* **1997**, *97*, 2267. (b) Lash, T. D. *Angew. Chem., Int. Ed.* **2000**, *39*, 1763. (c) Furuta, H.; Maeda, H.; Osuka, A. *Chem. Commun.* **2002**, 1795. (d) Sessler, J. L.; Seidel, D. *Angew. Chem., Int. Ed.* **2003**, *42*, 5134. (e) Ghosh, A. *Angew. Chem., Int. Ed.* **2004**, *43*, 1918. (f) Chadrashekar, T. K.; Venkatraman, S. *Acc. Chem. Res.* **2003**, *36*, 676.

(2) (a) Sessler, J. L.; Tomat, E.; Mody, T. D.; Lynch, V. M.; Veauthier, J. M.; Mirsaidov, U.; Markert, J. T. *Inorg. Chem.* **2005**, *44*, 2125. (b) Sessler, J. L.; Maeda, H.; Mizuno, T.; Lynch, V. M.; Furuta, H. *J. Am. Chem. Soc.* **2002**, *124*, 13474. (c) Weghorn, S. J.; Sessler, J. L.; Lynch, V.; Baumann, T. F.; Sibert, J. W. *Inorg. Chem.* **1996**, *35*, 1089.

(3) (a) Shin, J.-Y.; Furuta, H.; Yoza, K.; Igarashi, S.; Osuka, A. *J. Am. Chem. Soc.* **2001**, *123*, 7190. (b) Shimizu, S.; Shin, J.-Y.; Furuta, H.; Ismael, R.; Osuka, A. *Angew. Chem., Int. Ed.* **2003**, *42*, 78. (c) Srinivasan, A.; Ishizuka, T.; Osuka, A.; Furuta, H. *J. Am. Chem. Soc.* **2003**, *125*, 878. (d) Mori, S.; Osuka, A. *J. Am. Chem. Soc.* **2005**, *127*, 8030. (e) Hata, H.; Kamimura, Y.; Shinokubo, H.; Osuka, A. *Org. Lett.* **2006**, *8*, 1169. (f) Anand, V. G.; Saito, S.; Shimizu, S.; Osuka, A. *Angew. Chem., Int. Ed.* **2005**, 44, 7244.

(4) (a) Chandrasekhar, V.; Nagendran, S.; Azhakar, R.; Kumar, M. R.; Srinivasan, A.; Ray, K.; Chandrashekar, T. K.; Madhavaiah, C.; Verma, S.; Priyakumar, U. D.; Sastry, G. N. *J. Am. Chem. Soc.* **2005**, *127*, 2410. (b) Anand, V. G.; Pushpan, S. K.; Venkatraman, S.; Narayanan, S. J.; Dey, A.; Chandrashekar, T. K.; Roy, R.; Joshi, B. S.; Deepa, S.; Sastry, G. N. *J. Org. Chem.* **2002**, *67*, 6309. (c) Srinivasan, A.; Kumar, R. M.; Pandian, R. P.; Mahajan, S.; Pushpan, S. K.; Sridevi, B.; Narayanan, S. J.; Chandrashekar, T. K. *J. Porphyrins Phthalocyanines* **1998**, *2*, 305. (d) Srinivasan, A.; Reddy, V. M.; Narayanan, S. J.; Sridevi, B.; Pushpan. S. K.; Ravikumar, M.; Chandrashekar, T. K. *Angew. Chem., Int. Ed. Engl.* **1997**, *36*, 2598.

(5) (a) Chen, Z.; Wannere, C. S.; Corminboeuf, C.; Puchta, R.; Schleyer, P. v. R. *Chem. Rev.* **2005**, *105*, 3842. (b) Cyrañski, M. K. *Chem. Rev.* **2005**, *105*, 3773. (c) Raczyńska, E. D.; Kosińska, W.; Ośmiałowski, B.; Gawinecki, R. *Chem. Rev.* **2005**, *105*, 3561. (d) De Proft, F.; Geerlings, P. *Chem. Rev.* **2001**, *101*, 1451. (e) Balaban, A. T.; Oniciu, D. C.; Katritzky, A. R. *Chem. Rev.* **2004**, *104*, 2777. (f) Cyrañski, M. K.; Krygowski, T. M.; Katritzky, A. R.; Schleyer, P. v. R. *J. Org. Chem.* **2002**, *67*, 1333. (g) Schleyer, P. v. R. *Chem. Rev.* **2001**, *101*, 1115. (h) Gomes, J. A. N. F.; Mallion, R. B. *Chem. Rev.* **2001**, *101*, 1349. (i) Katritzky, A. R.; Jug, K.; Oniciu, D. C. *Chem. Rev.* **2001**, *101*, 1421. (j) Mitchell, R. H. *Chem. Rev.* **2001**, *101*, 1301. (k) Schleyer, P. v. R.; Maerker, C.; Dransfeld, A.; Jiao, H.; Hommes, N. J. R. v. E. *J. Am. Chem. Soc.* **1996**, *118*, 6317.

 10.1021/ja064773k CCC: $33.50

Chart 1. Molecular Structures of Expanded Porphyrins Considered in This Study

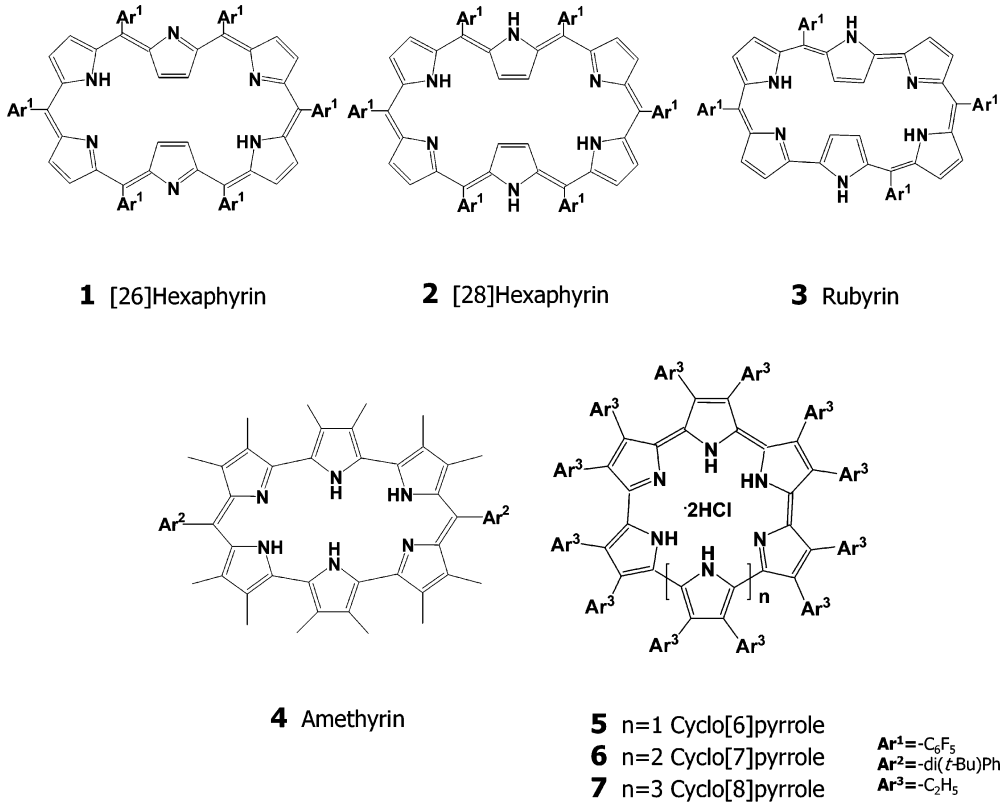

relationship between structure and electronic character, more sophisticated experimental and theoretical methods are needed if the issues of aromaticity in expanded porphyrins and, ultimately, related heteroannulene systems are to be more fully understood. In this report, a detailed comparison of the photophysical properties of a series of expanded porphyrins containing six ([26]hexaphyrin (**1**), [28]hexaphyrin (**2**), rubyrin (**3**), amethyrin (**4**), cyclo[6]pyrrole (**5**)), seven (cyclo[7]pyrrole, **6**) and eight (cyclo[8]pyrrole, **7**) pyrrole rings is presented. These systems, chosen because of their relative conformational rigidity, have been investigated by various time-resolved spectroscopic techniques, as well as through femtosecond Z-scan measurements. Based on these analyses, we have found that a simple, first-order relationship exists between the excited-state dynamics and various calculated and observed molecular features associated with (anti)aromaticity, including Nucleus-Independent Chemical Shift (NICS) values, the number of π-electrons, π-conjugation pathway, and structural planarity. Particularly noteworthy was the correlation between the calculated NICS values, obtained from GIAO/6-31G* calculations, and the two-photon absorption (TPA) coefficients determined using the femtosecond Z-scan method. Based on these findings, we suggest that various photophysical properties, most notably the TPA coefficients, can provide a quantitative experimental measure of aromaticity in various aromatic and antiaromatic macrocyclic π-conjugated systems.

Although long appreciated as being potentially informative, detailed optical studies of expanded porphyrins have hitherto been few in number. One of the key limitations to carrying out such studies is that many of the systems in question absorb and emit in the NIR (near-infrared) spectral region. However, recent advances have led to the development of the needed light sources and detection systems. This has permitted NIR absorption and emission studies, as well as femtosecond TPA measurement, to be carried out in the case of several expanded porphyrins. Indeed, two of our groups have recently applied these optical methods to the study of a matched pair of hexapyrrolic expanded porphyrins [26]- and [28]hexaphyrin (**1** and **2**). This study included determinations of both the photophysical and nonlinear optical (NLO) properties, as well as an analysis of the findings in the context of such easy-to-appreciate parameters as structural planarity, number of π-electrons, and aromaticity.[6] It also led to the tentative prediction that the TPA values could be used as a simple experimental marker of aromaticity. However, it was also recognized that support for this potentially far-reaching conclusion would require more extensive experimental and theoretical analyses. We have thus expanded our study to include a number of oligopyrrolic systems containing not only six but also seven and eight pyrrole rings, as well as 22, 24, 26, 28, and 30 π-electrons.

The systems chosen for the present study are shown in Chart 1 and involve representative hexa-, hepta-, and octapyrrolic systems recently reported in the literature.[6−9] Starting from [26]-hexaphyrin **1**,[3a,6] these expanded porphyrins may be classified according to the connectivity of the pyrrole rings. Rubyrin **3**

(6) (a) Ahn, T. K.; Kwon, J. H.; Kim, D. Y.; Cho, D. W.; Jeong, D. H.; Kim, S. K.; Suzuki, M.; Shimizu, S.; Osuka, A.; Kim, D. *J. Am. Chem. Soc.* **2005**, *127*, 12856. (b) Neves, M. G. P. M. S.; Martins, R. M.; Tomé, A. C.; Silvestre, A. J. D.; Silva, A. M. S.; Félix, V.; Drew, M. G. B.; Cavaleiro, J. A. S. *Chem. Commun.* **1999**, 385.

(7) (a) Shimizu, S.; Taniguchi, R.; Osuka, A. *Angew. Chem.* **2005**, *44*, 2225. (b) Sessler, J. L.; Morishima, T.; Lynch, V. *Angew. Chem.* **1991**, *30*, 977.

(8) (a) Sessler, J. L.; Weghorn, S. J.; Hiseada, Y.; Lynch, V. *Chem.—Eur. J.* **1995**, *1*, 56. (b) Hannah, S.; Seidel, D.; Sessler, J. L.; Lynch, V. *Inorg. Chim. Acta* **2001**, *317*, 211.

(9) Köhler, T.; Seidel, D.; Lynch, V.; Arp, F. O.; Ou, Z.; Kadish, K. M.; Sessler, J. L. *J. Am. Chem. Soc.* **2003**, *125*, 6872.

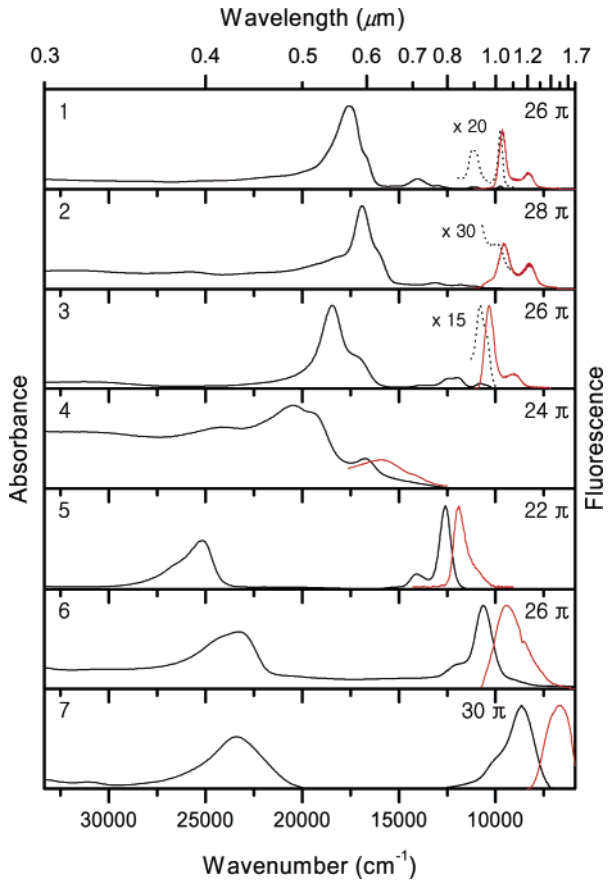

Figure 1. Steady-state absorption and emission spectra of **1**−**3** in toluene and **4**−**7** in CH_2Cl_2, measured in UV−vis−NIR region. Emission spectra were obtained by exciting **1**−**3** and **5**−**7** with a CW He−Cd laser at 442 nm in NIR region. The emission spectrum of **4** was obtained via excitation at several wavelengths with commercial spectrophotometer in vis region.

(formally [26]hexaphyrin(1.1.0.1.1.0)),[7] for instance, can be considered to be an analogue of [26]hexaphyrin(1.1.1.1.1.1) from which two *meso*-bridged carbons have been removed. Likewise, amethyrin **4** (formally [24]hexaphyrin(1.0.0.1.0.0))[8] can be formed by "extracting" two additional *meso*-bridged carbons from rubyrin, whereas cyclo[6]pyrrole **5** (formally [22]-hexaphyrin(0.0.0.0.0.0)),[9] results from a process wherein the last two *meso*-bridged carbons in amethyrin are "removed". Cyclo[7]pyrrole **6** (formally [26]heptaphyrin(0.0.0.0.0.0.0)) and cyclo[8]pyrrole **7** (formally [30]octaphyrin(0.0.0.0.0.0.0.0)) are homologues of cyclo[6]pyrrole that likewise contain no bridging *meso* carbon atoms. While known for several years, to the best of our knowledge, in no cases has the photophysics of these systems been investigated in detail. A first goal of this work was thus to carry out such a study, while a second was to correlate the putative nonlinear optical (NLO) properties of these various expanded porphyrins with such key parameters as aromaticity/antiaromaticity and structural planarity as inferred from the corresponding optimized molecular geometries. In accord with what was inferred from our previous study of **1** and **2**, a strong correlation between electronic structure and excited-state optical properties was indeed found.

Results and Discussion

Steady-State Absorption and Fluorescence Spectra. The steady-state absorption and fluorescence spectra of a series of expanded porphyrins, specifically **1**−**7** (Figure 1), were recorded from the visible to the NIR region in toluene for **1**−**3** and in CH_2Cl_2 for **4**−**7**. As a general rule, the spectral features were found to be significantly red-shifted compared to what is seen in 18 π-electron porphyrins, as would be expected in light of the enhanced π-conjugation pathways (Figure 1).[10]

Overall, the absorption spectra exhibit two apparent bands, presumably originating from intense S_0-S_2 and relatively weaker S_0-S_1 transitions in **1**−**3** and, conversely, weaker S_0-S_2 and relatively strong S_0-S_1 transitions in **5**−**7**. This leaves **4** as a notable exception; this system exhibits broad and featureless absorption bands in the range 300−500 nm, which we consider a diagnostic reflection of the nonaromatic nature of the molecule. To a first approximation, the fluorescence spectra appear as the mirror images of the corresponding absorption spectra. Key absorption and emission features and the relevant Stokes shifts are summarized in Table 1.

In contrast to the lack of disparity seen in their respective absorption spectra, notable differences were seen in the fluorescence emission spectra of **1** and **2**. Whereas a small Stokes shift is seen in the emission spectrum of the aromatic hexaphyrin **1**, its reduced congener **2** exhibits broad features in its emission spectrum, with a relatively large Stokes shift also being observed. We interpret these differences in terms of the presence of conformational heterogeneities in **2** that arise from geometrical changes induced by electronic relaxation within the excited state that are greater than those seen in the case of **1**.[6]

Among the hexapyrrolic macrocycles (**1**−**5**), only **4** exhibits significantly broad absorption and fluorescence bands in the visible region. In this case, there is no clear-cut discrimination between the S_1 and S_2 transitions, and a large Stokes shift, the biggest within the present series of compounds, is seen.

The steady-state absorption and fluorescence spectra of **5**−**7** show a systematic red shift of the lowest energy bands into the NIR region as the number of π-electrons increases. The spectral bandwidths and the Stokes shifts of compounds **5**−**7** likewise exhibit a systematic trend in parallel with the increasing number of π-electrons, a finding that can be interpreted in terms of a narrower conformational distribution and smaller structural changes between the ground and excited states in **5** compared to **6** and **7**. The differences in steric hindrance between the pyrrole rings induced by totally symmetric breathing modes, coupled with the slight loss in planarity associated with an increase in the number of pyrrole rings, likely determine the extent of structural relaxation in **5**−**7**.[11]

Geometry Optimization and Quantitative Analysis of Aromaticity. NICS (Nucleus-Independent Chemical Shift) values are a well-known parameter used to evaluate aromaticity that is recognized for its simplicity and efficiency.[5] Although quantitative measures of aromaticity for many five- and six-membered ring systems have been documented using this approach, corresponding NICS studies for larger π-conjugation systems, such as porphyrins, are scarce.[12] Moreover, the use of NICSs to quantify the putative aromaticity of expanded porphyrins has not, to the best of our knowledge, been previously attempted. Given this, we have calculated the NICS values for

(10) Yoon, M.-C.; Jeong, D. H.; Cho, S.; Kim, D.; Rhee, H.; Joo, T. *J. Chem. Phys.* **2003**, *118*, 164.
(11) Cho, H. S.; Kim, S. K.; Kim, D.; Fujiwara, K.; Komatsu, K. *J. Phys. Chem. A* **2000**, *104*, 9666.
(12) (a) Steiner, E.; Fowler, P. W. *Org. Biomol. Chem.* **2004**, *2*, 34. (b) Furuta, H.; Maeda, H.; Osuka, A. *J. Org. Chem.* **2001**, *66*, 8563.

Table 1. Number of π-electrons,[a] Band Maxima of Absorption and Fluorescence Spectra,[b–d] Stokes Shifts,[e] NICS(0) Values,[f] Aspect Ratios (AR),[g] TPA Cross-Section Values ($\sigma^{(2)}$),[h] and Singlet and Triplet Excited-State Lifetimes[i,j] of **1**−**7**

molecules			no. of π e^{-a}	λ_{abs}[b,c] (nm)	λ_{fl}[d] (nm)	ΔE_{Stokes}[e] (cm^{-1})	NICS[f] (ppm)	AR[g]	$\sigma^{(2)}$[h] (GM)	τ_S[i] (ps)	τ_T[j] (μs)
1	[26]hexaphyrin	(1.1.1.1.1.1)	26	567,[b] 1018[c]	1036	171	−14.3	1.44	9890[s]	100[s]	1.8[s]
2	[28]hexaphyrin	(1.1.1.1.1.1)	28	594,[b] 1009[c]	1040	295	+43.5	1.44	2600[s]	26[s]	0.04[s]
3	rubyrin	(1.1.0.1.1.0)	26	543,[b] 926[c]	968	469	−15.8	1.23	9080[h]	560[l]	146[o]
4	amethyrin	(1.0.0.1.0.0)	24	489,[b] 598[c]	632	900	+17.1	1.17	3100[i]	110[m]	—[p]
5	cyclo[6]pyrrole	(0.0.0.0.0.0)	22	398,[b] 794[c]	842	718	−11.4	1	2100[j]	430[n]	16[q]
6	cyclo[7]pyrrole	(0.0.0.0.0.0.0)	26	430,[b] 940[c]	1060	1204	−11.6	1	2350[k]	6.6[n]	4[r]
7	cyclo[8]pyrrole	(0.0.0.0.0.0.0.0)	30	427,[b] 1155[c]	1496	1974	−12.3	1	3030[k]	0.7[n]	—[p]

[a] Number of π-electrons. [b] Absorption wavelength maxima at B-like bands. [c] Absorption wavelength maxima at Q-like bands. [d] Fluorescence wavelength maxima. [e] Stokes shifts, that is, energy gaps between c and d. [f] Calculated at the ring center, NICS(0). [g] Calculated from optimized geometry. [h] Excitation at 1050 nm. [i] Excitation at 800 nm. [j] Excitation at 1550 nm. [k] Excitation at 1600 nm. [l] Pumped and probed at 550 and 650 nm, respectively. [m]Measured by fluorescence decay using TCSPC. Amethyrin in CH_2Cl_2 was excited at 410 nm, and the fluorescence was monitored at several wavelengths from 580 to 630 nm. [n] Pumped and probed at 400 and 570 nm, respectively. [o] Pumped and probed at 532 and 630 nm, respectively. [p] Not detected. [q] Pumped and probed at 800 and 550 nm, respectively. [r] Pumped and probed at 900 and 550 nm, respectively. [s] Reference 6a.

1−**7** at the ring center, NICS(0), from the energy minimized molecular structures using a Gaussian ab initio method at the B3LYP level, employing the GIAO (Gauge-Including Atomic Orbital) with the 6-31G* basis set. In these calculations, all peripheral substituents were ignored. This simplified the task of assigning the number of π-electrons participating in the π-conjugation pathways giving rise to potentially observable magnetic shielding/deshielding effects.

As shown in Table 1, the calculated NICS(0) values are negative for the presumed-to-be-aromatic compounds (**1**, **3**, **5**, **6**, and **7**) and positive for the putative antiaromatic species (**2** and **4**). Such findings are fully consistent with the aromaticity/antiaromaticity predictions that would be obtained by extending Hückel's original $[4n + 2]$ rule to encompass large heteroannulene systems, such as **1**−**7**. In this context it is to be noted that a strict counting of the total number of π-electrons is not always sufficient for determining the predicted Hückel aromaticity of a system because often there is a superposition of several pathways.[13] On the other hand, the presence of a conjugated $[4n + 2]$ π-electron periphery provides a remarkably good, albeit qualitative, predictor of aromaticity in oligopyrrolic macrocyclic systems.

The formal addition of 2 molar equiv of hydrogen into **1** (to produce **2**) leads to a reversal in the sign of the NICS values from negative (aromaticity) to positive (antiaromaticity). This is as expected, given the change in the number of π-electrons in the conjugation pathway (26 and 28). However, in the case of **2**, the experimental chemical shift values, as determined by ^{1}H NMR spectroscopy, reveal that **2** is best considered as being nonaromatic, rather than antiaromatic. In a sense, the results obtained from the ^{1}H NMR spectroscopic analyses and the NICS calculations contradict each other. However, it is important to note that the magnetic deshielding predicted by the NICS calculation reflects the ring current produced by the full complement of π-electrons delocalized over the entire π-conjugation pathway. Conversely, the chemical shift of a given signal within the ^{1}H NMR spectrum depends on the local electronic environment for the proton or protons in question. In this context it is interesting to consider that individual protons in **2**, although ostensibly nonaromatic (as inferred from their respective chemical shift values), could nonetheless be contained within a system displaying a net antiaromatic ring current. In particular, it is suggested that **2** may be nonaromatic in character as judged by the short-range shielding contributions of protons yet nonetheless be antiaromatic when the full long-range contribution of the delocalized π-electrons (manifest in ring current effects) is taken into consideration.[13] Although we have not yet clarified the reason [28]hexaphyrin shows spectral features that make it best designated as nonaromatic, such a finding could reflect its structural flexibility. Consistent with this conclusion is the finding that [28]hexaphyrins that are constrained as conformationally rigid (e.g., via formation of the corresponding Au(III) complexes) display distinctly antiaromatic character.[3d]

A different feature of the NICS calculations is revealed via a comparison between **1** and **3**. Although both macrocycles contain the same number of π-electrons (26), **3** is actually smaller than **1** (in terms of ring size) and displays a slightly larger NICS value. Such a finding leads to the conclusion that the NICS value is only weakly dependent on ring size and is better viewed as being a gauge of net aromaticity. Consistent with this latter conclusion is the finding that the NICS parameter for **6**, also a net 26 π-electron system, is smaller than that for **3**.

Two-Photon Absorption (TPA) Properties. Two-photon absorption (TPA) is a nonlinear optical process, occurring under an intense electric field usually generated by pulse lasers with simultaneous absorption of two or more photons by a single chromophore to produce a high-energy excited state. The TPA cross-section thus provides a measure of a third-order nonlinear optical process produced in response to an external electric field. Within the context of such general considerations, the number of π-electrons and/or the molecular geometry associated with the static and dynamic polarizability have been established as determining factors in controlling nonlinear optical susceptibility, at least within simple molecular systems.[14]

Given the defining roles of molecular electronics and structure in regulating NLO effects, expanded porphyrins are of particular interest since both of these key parameters can, at least in principle, be easily controlled. Thus, with the matched set of compounds **1**−**7** in hand, we performed femtosecond Z-scan experiments to probe the nature and extent of the presumed nonlinear optical response (Supporting Information). The excita-

(13) (a) Aihara, J. *J. Am. Chem. Soc.* **2006**, *128*, 2873. (b) Jusélius, J.; Sundholm, D. *Phys. Chem. Chem. Phys.* **2000**, *2*, 2145.

(14) (a) Lee, S.; Thomas, K. R. J.; Thayumanavan, S.; Bardeen, C. J. *J. Phys. Chem. A* **2005**, *109*, 9767. (b) Day, P. N.; Nguyen, K. A.; Pachter, R. *J. Phys. Chem. A* **2005**, *109*, 1803. (c) Yang, W. J.; Kim, D. Y.; Kim, C. H.; Jeong, M.-Y.; Lee, S. K.; Jeon, S.-J.; Cho, B. R. *Org. Lett.* **2004**, *6*, 1389.

tion wavelengths for the open aperture experiments were in the NIR region (see the footnotes in Table 1); this is a spectral region where the contribution from linear absorption effects is nearly negligible. In our previous study, we compared the TPA values of **1** and **2** and explained that the smaller TPA value seen for **2** reflects its decreased molecular planarity, as well as its reduced aromatic character, as determined by the number of π-electrons (Hückel's [$4n + 2$] rule) present in the system.[6a]

In our current studies, we found that **3** exhibits a TPA value that is similar to **1** (both 26 π-electron systems) while compound **4** (a 24 π-electron system) is characterized by a TPA that is much smaller than that displayed by either **1** or **3**. This finding is consistent with previous investigations involving the NLO properties of smaragdyrin analogues by Chandrashekar et al.; here, a larger TPA value was seen in the *para*-linked isomer than in the corresponding *meta*-linked system, a finding that was attributed to the lack of complete π-conjugation in the *meta* isomer.[15] An important ancillary conclusion that could be drawn from this prior work is that the extent of effective π-conjugation is strongly correlated with the molecular geometry. This then provides a means for interpreting what is seen in **4**. In particular, we suggest that the TPA values, and hence optical nonlinearity, should depend on the aspect ratio (A.R., long-axis/short-axis), which in turn can be estimated from the optimized molecular geometry. In the case of the hexapyrrolic systems being considered in this study, consecutive synthetic "removal" of a pair of *meso*-carbons on passing from **1** (A.R. = 1.44) to **3** (A.R. = 1.23) and then to **4** (A.R. = 1.17) should give rise to TPA values that decrease in sequence such that **1** > **3** > **4**.

Consistent with this postulate is the finding discussed in a previous report that the TPA values of fused zinc(II) porphyrin arrays (**T*N***) with "fully conjugated" π-electron systems increase as the π-conjugation pathway becomes elongated.[16] Although this observation most likely reflects an enhanced π-conjugation effect, the molecular geometry, as quantified in the aspect ratio, can also be an important factor in determining TPA values. In fact, oligoporphyrins linked within a squarelike arrangement to provide a two-dimensional π-extended array (referred to as a porphyrin "sheet") invariably display a small (i.e., near-unity) aspect ratio. As a consequence the TPA value of the porphyrin sheet is much smaller than that of the corresponding linear fused arrays.[17]

In the present study we found that the antiaromatic systems **2** and **4** show smaller TPA values than **1** and **3**, even though the aspect ratio of **2** is roughly the same as that of **1**, and that of **4** is slightly smaller than that of **3**. We think that this is because molecules tend to avoid antiaromatic situations (28 and 24 π-electrons for **2** and **4**, respectively) by adopting, in the present cases, distorted "tub" structures. These latter systems then give rise to small TPA values as a result of the reduced planarity.

Furthermore, as the overall ring size increases, i.e., upon going from **5** to **7**, the TPA values also increase. Considering that TPA values increase with increasing polarizability within a given series of molecules, as well as the well-established linear relationship between polarizability and softness, leads us to interpret the larger TPA values seen for **7** relative to **6** and **5** in terms of Koopmans' theorem,[18]

$$\eta = \frac{\epsilon_L - \epsilon_H}{2} \tag{2}$$

where η is the hardness, and ϵ_L and ϵ_H are the lowest unoccupied and highest occupied molecular orbital energies, respectively. As illustrated by the smaller HOMO−LUMO energy gap observed in the steady-state absorption spectra and molecular orbital calculations, the hardness of **7** is smaller than that of **5** or **6**. We therefore suggest that the larger TPA value seen in **7** compared to **5** and **6** arises from the greater softness, which results in an increased polarizability in the case of **7**.

To summarize the above discussion, it is proposed that both features of (1) aromaticity and (2) the specifics of the π-conjugation pathway, as determined by molecular shape, play important roles in determining the TPA values.

Support for the first effect (aromaticity) comes from a comparison between the aromatic system **1** and its reduced, antiaromatic congener **2**, as well as by a similar comparison between the aromatic **3** and the antiaromatic **4**. In both cases, the less aromatic system, as judged from an analysis of the number of π-electrons and supporting NICS calculations, displayed the lower TPA values. While not strictly analogous to these "pairs", the fact that the highly antiaromatic cyclooctatetraene core (NICS(0) = +61.7) found in the center of the hitherto reported porphyrin sheet gives rise to low TPA values further supports this generalization.

Support for the second effect (specifics of the molecular structure) comes from an analysis of the matched set consisting of **1**, **3**, and **6**. These three macrocycles have the same number of π-electrons (26), but macrocycle **1** has the highest aspect ratio and displays the largest TPA value within the series. The fact that a larger TPA value was seen for the fused porphyrin linear tetramer **T4**, as compared to the porphyrin sheet, in previous work, also lends credence to the conclusion that the aspect ratio and hence structure correlate with TPA values. Similar support comes from the work of Anderson et al., wherein a higher TPA value was seen in the case of various π-conjugated zinc(II) porphyrin dimers linked via the *para* position of an intervening spacer, rather through a *meta* substituted link.[19]

Singlet and Triplet Excited-State Lifetimes. To explore the excited singlet and triplet state properties of **1**−**7** and to obtain insights into the corresponding energy relaxation processes, femtosecond and nanosecond transient absorption experiments were performed. These studies were carried out at room temperature in toluene solution in the case of **1**−**3** and in CH_2Cl_2 solution for **4**−**7** (Supporting Information). The resulting decays were fit to give the parameters summarized in Table 1.

In our previous study, involving an analysis of [26] and [28]-hexaphyrins **1** and **2**, we interpreted the singlet and triplet excited-state lifetimes using conformational dynamics as re-

(15) Misra, R.; Kumar, R.; Chandrashekar, T. K.; Nag, A.; Goswami, D. *Org. Lett.* **2006**, 8, 629.
(16) (a) Ahn, T. K.; Kim, K. S.; Kim, D. Y.; Noh, S. B.; Aratani, N.; Ikeda, C.; Osuka, A.; Kim, D. *J. Am. Chem. Soc.* **2006**, *128*, 1700. (b) Kim, D. Y.; Ahn, T. K.; Kwon, J. H.; Kim, D.; Ikeue, T.; Aratani, N.; Osuka, A.; Shigeiwa, M.; Maeda, S. *J. Phys. Chem. A* **2005**, *109*, 2996.
(17) Nakamura, Y.; Aratani, N.; Shinokubo, H.; Takagi, A.; Kawai, T.; Matsumoto, T.; Yoon, Z. S.; Kim, D. Y.; Ahn, T. K.; Kim, D.; Muranaka, A.; Kobayashi, N.; Osuka, A. *J. Am. Chem. Soc.* **2006**, *128*, 4119.
(18) (a) Padmanabhan, J.; Parthasarathi, R.; Subramanian, V.; Chattaraj, P. K. *J. Phys. Chem. A* **2005**, *109*, 11043. (b) Chattaraj, P. K.; Fuentealba, P.; Gomez, B.; Contreras, R. *J. Am. Chem. Soc.* **2000**, *122*, 348.
(19) Drobizhev, M.; Stepanencko, Y.; Dzenis, Y.; Karotki, A.; Rebane, A.; Taylor, P. N.; Anderson, H. L. *J. Phys. Chem. B* **2005**, *109*, 7223.

vealed by temperature-dependent femtosecond transient absorption experiments.[6a] The shorter excited-state lifetime of **2** relative to **1** was thus attributed to the perturbed electronic structures induced by antiaromaticity resulting from the $4n$ π-electron configuration of **2**. In other words, the excited-state dynamics could be correlated with the aromaticity/antiaromaticity and thus related to molecular geometry.

In the present study, we have found that "removing" two *meso*-bridged carbons from **1** (1.1.1.1.1.1) to make **3** (1.1.0.1.1.0) leads to a significant increase in both the singlet and triplet excited-state lifetimes, even though both compounds have the same number of π-electrons (26) in their most favorable conjugation pathway. We interpret this result in terms of the rigid and stabilized molecular structure of **3**, which should make it the most conformationally favored among the hexapyrrolic systems included in this study. In other words, the longer excited-state lifetimes of **3** (relative to **1**) support the notion that Hückel-type $[4n + 2]$ aromaticity is going to be manifest to a greater extent within those systems that can adopt easily rigid, planar structures without having to pay an excessive energetic price in terms of steric distortion.

The relative stability of **3** becomes further apparent when comparisons are made to its congener **4** (a 24 π-electron system) from which two *meso*-bridge carbon atoms have been eliminated. The resulting system compared to **3** exhibits a shorter S_1 state lifetime, a result that is most readily interpreted in terms of structural deformation induced by the antiaromaticity present in **4**. Consistent with this was the finding that we were unable to detect a T−T absorption signal in the case of **4**; presumably, the structural deformation induced so as to mitigate the effects of Hückel-type antiaromaticity effects gives rise to a shorter excited-state lifetime. This putative structural deformation was also reflected in the absorption and fluorescence spectra, wherein broad spectral features and a larger Stokes shift are observed, along with a positive NICS value.

Interestingly, as two additional *meso*-bridging carbon atoms are removed (i.e., on passing from **4** to the [22]hexaphyrin-(0.0.0.0.0.0) **5**), longer singlet and triplet state lifetimes are once again observed; this is rationalized in terms of the "reappearance" of aromaticity (**5** is a 22 π-electron system) and the associated structural stabilization.

As the number of pyrrole rings increases, as it does within the matched set **5**, **6**, and **7**, the singlet and triplet excited-state lifetimes decrease. Decreasing band gap energies between the HOMO and LUMO levels are seen. Likewise, increasing Stokes shifts are observed. Furthermore, the singlet excited state of **7** proved exceedingly short. In fact, it proved too short-lived (τ_s = 0.7 ps) to populate the triplet excited state. Thus, no triplet state decay processes could be monitored in the case of **7**. Taken in concert, these findings are thought to reflect the increased conformational flexibility expected upon going from **5** to **7**, as well as the presence of extended π-conjugation pathways. In this context, it is interesting to note that the compounds **1**, **3**, and **6** have the same number of π-electrons (26), resulting in similar band gap energies. Nonetheless, the singlet excited-state lifetime of **6** is considerably shorter than those of **1** and **3**. Again, this is interpreted in terms of steric constraints within a system that is "too small" to accommodate both the intraring "bite angles" and the beta-pyrrolic substituents without undergoing some slight structural deformation (e.g., deviation from planarity).

Overall, by comparing the singlet and triplet excited-state lifetimes in **1**−**7**, we are able to note several systematic tendencies that are useful in terms of rationalizing and predicting the excited state lifetimes. First, the nature of the connectivity is important in the case of the hexapyrrolic systems, and second, within an analogous series of aromatic expanded porphyrins, the number of pyrroles, as well as the way they are connected to one another, is important. As a result, the differences between ostensibly similar macrocycles can be profound.

Conclusions

In this work, we have explored the nonlinear optical properties and excited-state dynamics of various expanded porphyrins as an extension of our previous comparative study of [26] and [28]-hexaphyrins. Based on the steady-state absorption and fluorescence spectral features observed in the UV−NIR region and the results of quantitative analyses of aromaticity using NICS calculations, the excited-state dynamics of expanded porphyrins **3**−**7** can be predicted qualitatively from the corresponding molecular structures as defined by the number of bridging *meso*-carbon atoms. Using femtosecond Z-scan methods, the nonlinear optical properties of this matched set of congeners was also investigated, from which strategies to enhance TPA values were inferred. In particular, it is predicted that enhanced nonlinear optical properties will be seen when (i) the effective π-conjugation is accompanied by a larger number of π-electrons as long as Hückel's generalized $[4n + 2]$ rule for aromaticity is satisfied, (ii) the specific molecules in question are flat and rigid, and (iii) the molecular structures are best described as rectangular, rather than square or circular, so as to increase the polarizability along the long molecular axis.

Within the assumptions inherent in Hückel's $[4n + 2]$ rule, NICS calculations can be used to determine aromaticity or antiaromaticity in a quantitative manner according to the number of π-electrons. However, such assessments are strictly theoretical. On the other hand, the combination of experimental femtosecond Z-scan measurements coupled with NICS calculations leads us to suggest that, at least within an appropriately matched set of molecular structures, the experimentally derived TPA values can be regarded as an empirical measure of aromaticity. To the extent this is true, the parameter could emerge as one that could complement others, such as ring current effects and UV−vis spectroscopic features (λ_{max}, ϵ), which are currently being used for this purpose. Accordingly, further investigations into the relationship between NLO properties and aromaticity are now under way.

Experimental Section

Steady-State Absorption and Emission. Steady-state absorption spectra were acquired using a UV−vis−NIR spectrometer (Varian, Cary5000). Steady-state fluorescence spectra were recorded on a fluorescence spectrometer (Hitachi, FL2500). For the observation of near-infrared (NIR) emission spectra, a photomultiplier (Hamamatsu, R5108) and a lock-in amplifier (EG&G, 5210), combined with a chopper after laser excitation at 442 nm from a CW He−Cd laser (Melles Griot, OmNichrome 74) were used.

Time-Correlated Single Photon Counting. Time-resolved fluorescence was detected using a time-correlated single photon counting

(TCSPC) technique. A homemade cavity dumped Ti:Sapphire oscillator pumped by a CW Nd−YVO_4 laser (Coherent, Verdi) was used as the excitation light source; this provided ultrashort pulses (100 fs at full width half-maximum) and allowed for a high repetition rate (200−400 kHz). The output pulse of the oscillator was frequency-doubled with a second harmonic crystal. The TCSPC detection system consisted of a multichannel plate photomultiplier (Hamamatsu, R3809U-51) with a cooler (Hamamatsu, C4878), a TAC (time-to-amplitude converter) (EG&G Ortec, 457), two discriminators (EG&G Ortec, 584 (signal) and Canberra, 2126 (trigger)), and two wideband amplifiers (Philip Scientific (signal) and a Mini Circuit (trigger)). A personal computer with a multichannel analyzer (Canberra, PCA3) was used for data storage and processing. The overall instrumental response function was about 60 ps (fwhm). A sheet polarizer, set at an angle complementary to the magic angle (54.7°), was placed in the fluorescence collection system. The decay fittings were made by using a least-squares deconvolution fitting process (LIFETIME program with an iterative nonlinear least-squares deconvolution procedure developed at the University of Pennsylvania).[20]

Femtosecond Transient Absorption. Measurements were made using a setup involving a dual-beam femtosecond time-resolved transient absorption spectrometer consisted of two independently tunable homemade optical parametric amplifiers (OPAs) pumped by a Ti:sapphire regenerative amplifier system (Spectra-Physics, Hurricane X) operating at 5 kHz repetition rate and an optical detection system. The OPAs were based on noncollinearly phase-matching geometry and easily color-tuned by controlling the delay between the white light continuum pulses and pump pulses. The generated visible OPA pulses had a pulse width of ∼35 fs and an average power of 10 mW at a 5 kHz repetition rate in the range 500−700 nm. The probe beam was split into two parts. One part of the probe beam was overlapped with the pump beam at the sample to monitor the transient (signal), while the other part of the probe beam was passed through the sample without overlapping the pump beam to compensate the fluctuation of the probe beam (reference). The time delay between pump and probe beams was carefully controlled by making the pump beam travel along a variable optical delay (Newport, ILS250). To obtain the time-resolved transient absorption difference signal at a specific wavelength, the monitoring wavelength was selected by using an interference filter. By chopping the pump pulses at 47 Hz, the modulated probe pulses as well as the reference pulses were detected by two separate photodiodes. The modulated signals of the probe pulses were measured by a gated integrator (SRS, SR250) and a lock-in amplifier (EG&G, DSP7265) and stored on a personal computer for further signal processing. The polarization angle between the pump and probe beams was set to the magic angle (54.7°) in order to obviate polarization-dependent signals.

Nanosecond Transient Absorption. Nanosecond transient absorption spectra were obtained using nanosecond flash photolysis methods.[6a] Specifically, an excitation pulse of 532 nm was generated from the second harmonic output of a Q-switched Nd:YAG laser (Continuum, Surelite). The duration of the excitation pulse was ca. 6 ns, and the pulse energy was ca. 2 mJ/pulse. A CW Xe lamp (150 W) was used as a probe light source for the transient absorption measurement. After passing through the sample, the probe light was collimated and then spectrally resolved using a 15 cm monochromator (Acton Research, SP150) equipped with a 600 groove/mm grating. The spectral resolution was about 3 nm for a typical transient absorption experiment. The light signal was detected via a photomultiplier tube (Hamamatsu, R928). For the temporal profile measurements, the output signal from the PMT was recorded using a 500 MHz digital storage oscilloscope (Tektronix, TDS3052). Because the triplet state dynamics of molecules in solution are strongly dependent on the solution oxygen concentration, efforts were made to remove oxygen rigorously by repeated freeze−pump−thaw cycles. To ensure reproducibility and reliability, the triplet state dynamics of a known standard, Zn(II)TPP (TPP = tetraphenylporphyrin), were first recorded in toluene under unaerobic conditions, giving a lifetime of 1 ms at room temperature. Because the concentration of molecules also affects significantly the excited triplet state lifetime (as the result of, e.g., triplet−triplet annihilation processes), efforts were also made to keep the concentration of the samples at or below 10^{-5} M. A relatively low photoexcitation density at 532 nm (produced by the second harmonic output of a Q-switched Nd:YAG laser) was also used.

Two-Photon Absorption Cross-Section ($\sigma^{(2)}$). The TPA experiments were performed using the open-aperture Z-scan method with 130 fs pulses from an optical parametric amplifier (Light Conversion, TOPAS) operating at a 5 kHz repetition rate using a Ti:sapphire regenerative amplifier system (Spectra-Physics, Hurricane). The laser beam was divided into two parts. One was monitored by a Ge/PN photodiode (New Focus) as the intensity reference, and the other was used for the transmittance studies. After passing through an $f = 10$ cm lens, the laser beam was focused and passed through a quartz cell. The position of the sample cell could be varied along the laser-beam direction (z-axis), so the local power density within the sample cell could be changed under a constant laser power level. The thickness of the cell is 1 mm. The transmitted laser beam from the sample cell was then probed using the same photodiode as used for reference monitoring. The on-axis peak intensity of the incident pulses at the focal point, I_0, ranged from 40 to 60 GW/cm. Assuming a Gaussian beam profile, the nonlinear absorption coefficient β can be obtained by curve fitting to the observed open aperture traces with the following equation:

$$T(z) = 1 - \frac{\beta I_0 (1 - e^{-\alpha_0 l})}{2\alpha_0 (1 + (z/z_0)^2)}$$

where α_0 is the linear absorption coefficient, l, the sample length, and z_0, the diffraction length of the incident beam. After obtaining the nonlinear absorption coefficient β, the TPA cross-section $\sigma^{(2)}$ (in units of 1 GM = 10^{-50} cm^4·s/photon·molecule) of a single solute molecule sample can be determined by using the following relationship:

$$\beta = \frac{\sigma^{(2)} N_A d \times 10^{-3}}{h\nu}$$

where N_A is the Avogadro constant, d is the concentration of the TPA compound in solution, h is Planck's constant, and υ is the frequency of the incident laser beam. So as to satisfy the condition of $\alpha_0 l \ll 1$, which allows the pure TPA $\sigma^{(2)}$ values to be determined using a simulation procedure, the TPA cross-section value of AF-50 was measured as a reference compound; this control was found to exhibit a TPA value of 50 GM at 800 nm.

Acknowledgment. The work at Yonsei University was financially supported by the Star Faculty Program of the Ministry of Education and Human Resources. The work at Kyoto University was supported by the CREST of JST. The work at the University of Texas at Austin was supported in part by the U.S. National Science Foundation (CHE 0515670 to J.L.S.).

Supporting Information Available: Preparation of **1**−**7**; molecular extinction coefficient of **1**−**7**; schematic conjugation pathways and NICS(0) values of **1**−**7**; S1-state decay profiles of **1**−**7**; T1-state decay profiles of **3**, **5**, and **6**; open-aperture femtosecond Z-scan traces of **3**−**7**. This material is available free of charge via the Internet at http://pubs.acs.org.

JA064773K

(20) Ahn, T. K.; Yoon, Z. S.; Hwang, I.-W.; Lim, J. K.; Rhee, H.; Joo, T.; Sim, E.; Kim, S. K.; Aratani, N.; Osuka, A.; Kim, D. *J. Phys. Chem. B* **2005**, *109*, 11223.